Magnetic form factor in $CeRu_2Si_2$ on crossing its metamagnetic transition

2001 J. Phys.: Condens. Matter 13 10901

(http://iopscience.iop.org/0953-8984/13/48/315)

INSTITUTE OF PHYSICS PUBLISHING JOURNAL OF PHYSICS: CONDENSED MATTER

J. Phys.: Condens. Matter **13** (2001) 10901–10909 PII: S0953-8984(01)29578-2

Magnetic form factor in $CeRu_2Si_2$ on crossing its metamagnetic transition

J-X Boucherle[1,5], F Givord[1,5,6], S Raymond[1], J Schweizer[1], E Lelièvre-Berna[2], P Lejay[3] and G Fillion[4]

[1] Département de Recherche Fondamentale sur la Matière Condensée-Service de Physique Statistique, Magnétisme et Supraconductivité-Magnétisme et Diffraction Neutronique (SPSMS-MDN), CEA/Grenoble, 38054 Grenoble Cedex 9, France
[2] Institut Laue Langevin, BP156, 38042 Grenoble Cedex 9, France
[3] CRTBT, CNRS, 166X, 38042 Grenoble Cedex 9, France
[4] Laboratoire Louis Néel, CNRS, 166X, 38042 Grenoble Cedex 9, France

E-mail: givord@drfmc.ceng.cea.fr

Received 10 October 2001
Published 16 November 2001
Online at stacks.iop.org/JPhysCM/13/10901

Abstract

The magnetic form factor of the heavy fermion compound $CeRu_2Si_2$ was measured by polarized neutron diffraction in the Pauli paramagnetic phase and above the metamagnetic transition. The magnetization density is characteristic of 4f electrons in both phases with an almost pure $|5/2, 5/2\rangle$ ground-state wavefunction. The only field effect observed in this experiment corresponds to a nonlinear variation of the magnetization of the 4f electrons.

1. Introduction

After two decades of intense experimental and theoretical studies on heavy fermion (HF) compounds, and even if a global picture has emerged, the extraordinary richness of these compounds (anomalous magnetism, metamagnetism, unconventional superconductivity) has hardly been grasped [1]. $CeRu_2Si_2$ is among the most extensively studied HF compounds as an archetypal Pauli paramagnet without any condensation into a magnetic or superconducting state down to the lowest temperature of 20 mK [2]. It is characterized by a large linear coefficient of specific heat $\gamma = 350$ mJ mol^{-1} K^{-2} together with an enhanced Pauli susceptibility and a T^2 law of resistivity below 1 K, all these features being described by the Landau–Fermi liquid theory.

A more striking feature of $CeRu_2Si_2$ is the nonlinear increase of its magnetization, M, with magnetic field, H. The occurrence of a sharp inflection in $M(H)$ for a magnetic field $H_m = 7.7$ T applied along the easy c-axis of the tetragonal structure, the so-called metamagnetic

[5] CNRS staff.
[6] Author to whom correspondence should be addressed.

transition, has attracted much experimental and theoretical interest. It is, in fact, a pseudo-metamagnetic transition since the ground state is paramagnetic. There is indeed no divergence of the bulk susceptibility at H_m but a sharp peak. Correspondingly, γ is also peaked at H_m indicating strong electronic effects. Large changes in the lattice properties corresponding to a quasi-collapse of the lattice are in evidence at H_m. Finally, antiferromagnetic spin fluctuations observed by inelastic neutron scattering (INS) are found to vanish at the metamagnetic transition. This transition is thus a cooperative effect between magnetic, lattice and electronic properties [2]. This behaviour is unique among HF systems, and the nature of the 4f electrons, itinerant versus localized, as a function of the applied magnetic field is still a subject of controversy. In this respect, dHvA experiments performed on both sides of H_m have been interpreted on the basis of two different models [3]. At low field, the 4f electrons are included in the quasi-particle band while in the high-field phase, a localized model is used to describe the data. In contrast, Hall effect measurements were interpreted on the basis of a continuous behaviour of heavy quasi-particles [4]. Concerning magnetization density fluctuations, an insight has been given by recent NMR/NQR experiments performed on Ru and Si sites [5, 6].

This has motivated us to study the metamagnetic transition of $CeRu_2Si_2$ by using neutron scattering which also probes magnetization density fluctuations, but on another time and space scale than NMR/NQR. This paper reports on static measurements of the form factor of the magnetization density in $CeRu_2Si_2$ on both sides of H_m obtained via polarized neutron diffraction. The INS experiments which aimed to study dynamical aspects have already been reported elsewhere [7].

2. Measurements

In order to investigate the location of the magnetic density, polarized neutron diffraction measurements were undertaken. The flipping ratio $R = I^+/I^- = (1+\Gamma)^2/(1-\Gamma)^2$ of a Bragg reflection $(h\,k\,l)$ yields the value of $F_M(h\,k\,l)$ through $\Gamma = F_M/F_N$, where F_N and F_M are the nuclear and magnetic structure factors, respectively. $F_M(h\,k\,l)$ are the Fourier components of the magnetization density $M(r)$. Very precise nuclear structure factors and a good knowledge of the extinction effects in the sample are then necessary to analyse polarized neutron data.

$CeRu_2Si_2$ crystallizes in the $I4/mmm$ space group with the lattice parameters $a = b = 4.196$ Å and $c = 9.797$ Å. The samples used in this study were cut from the large single crystal grown by the Czochralsky method [8] previously studied by INS experiments.

The crystal structure and the extinction effects were studied on a platelet ($4.6 \times 3.5 \times 0.8$ mm^3) at $T = 6.5$ K on the neutron four-circle diffractometer DN4 at the Siloé reactor (CEA/Grenoble). The wavelength was 1.18 Å. After averaging the reflections measured several times and the Friedel pairs, 106 non-equivalent reflections remained. A least-squares fitting program (MXD [9]) was used for the refinement of the crystal structure parameters; the scattering lengths b were taken from [10]. The Si position parameter (z_{Si}), the Debye–Waller thermal parameter B and populations on the different sites were refined. Due to the low temperature of the measurements, the use of anisotropic thermal parameters did not improve the agreement factor. The $\lambda/2$ contamination ($C_{\lambda/2}$) was also considered. This study revealed that the extinction effects were taken into account in a much better way by using the complete Becker–Coppens model [11] including primary extinction with two parameters (mosaicity g and block size t). All the refined parameters are given in table 1. The best results were obtained for a population on the Ce site slightly below 1. These structure parameters were then used to calculate F_N for processing the results of the polarized neutron measurements.

Table 1. Results of the refinement of the nuclear structure. The extinction parameters t (block size) and g (mosaicity) are defined as in [12]. The reliability factor is defined as $R_w = \sqrt{\sum_i p_i (I_i^{obs} - I_i^{calc})^2 / \sum_i p_i (I_i^{obs})^2}$ and $\chi^2 = \sum_i p_i (I_i^{obs} - I_i^{calc})^2 / (N_{obs} - N_{var})$ with $p_i = 1/\sigma_i^2$.

Site	x	y	z	b (fm)	Population	B (Å^2)
Ce (2a)	0	0	0	4.84	0.985(10)	0.04(5)
Ru (4d)	0	1/2	1/4	7.03	≡1.0	0.09(2)
Si (4e)	0	0	0.3648(1)	4.15	≡1.0	0.12(3)

$\lambda/2$ contamination	Extinction	Agreement
$C_{\lambda/2} \equiv 0.007$	$g = 600(50)$ rad^{-1}	$R_w = 3.12\%$
	$t = 11(2)$ μm	$\chi^2 = 9.6$

The polarized neutron experiments were carried out on the D3 diffractometer of the high flux ILL reactor. The sample was a single crystal platelet 5.4 × 3.8 × 0.8 mm^3 cut next to the crystal used for the crystallographic study. The magnetization curve of this crystal was measured at the Laboratoire Louis Néel (Grenoble) and is shown in figure 1. As for previous samples [2], it presents a transition around $H_m = 7.7$ T. Three sets of flipping ratios R were obtained with different fields applied along the easy c-axis: these correspond to experiments carried out in the paramagnetic phase at $H = 4.6$ T, where the magnetization is linear in field, in the high magnetization phase at $H = 9.5$ T, and in the transition region at $H = 7.8$ T. Experimental conditions are gathered in table 2. All measurements were performed at $T = 1.5$ K. For the experiment in $H = 4.6$ T, 208 flipping ratios R of 67 strong reflections were measured at several different wavelengths ($\lambda = 0.843$, 0.711, 0.545 and 0.420 Å), taking advantage of the ILL hot source, in order to optimize the extinction corrections [12,13]. A new refinement of the two extinction parameters g and t was performed from these R values, using for F_N the values previously calculated. The major role of the primary extinction (large value of t) is confirmed, but the new extinction parameters as found are somewhat different from those determined from the four-circle experiment (table 1). These discrepancies are attributed to the fact that the two determinations were performed on different single crystals. The final values used for the data analysis of the polarized neutron experiments are those deduced from the flipping ratios R refinements, that is $g = 110(170)$ rad^{-1} and $t = 26(6)$ μm. These parameters were then taken as input, together with experimental corrections.

3. Results

Among all the available reflections, some of them (seven reflections ($h\,k\,l = 0$) with h and k odd, and five reflections ($h\,k\,l = 1$)) have an extremely weak nuclear structure factor F_N (≈1 fm compared to 20–50 fm for other reflections). For these reflections, it then appeared impossible to deduce, with a satisfactory accuracy, the magnetic structure factor F_M from the flipping ratio R. So we decided to leave aside these reflections, and the number of remaining non-equivalent reflections is given in table 2.

A Fourier analysis using the three-dimensional (3D) maximum entropy (MaxEnt) technique [14–16] has been used to obtain the most probable magnetization distribution map compatible with the measured $F_M(h\,k\,l)$. The main advantage of the MaxEnt technique, compared to the classical Fourier synthesis, is that it makes no assumption concerning unmeasured Fourier components and takes into account the experimental uncertainties. The

Table 2. Experimental conditions for the various polarized neutron experiments.

H (T)	λ (Å)	l_{max}	Total number of reflections	Number of non-equivalent reflections
4.6	0.843	4	153	42
	0.711		63	
	0.545		65	
	0.420		13	
7.8	0.852	2	80	19
9.5	0.852	4	194	43

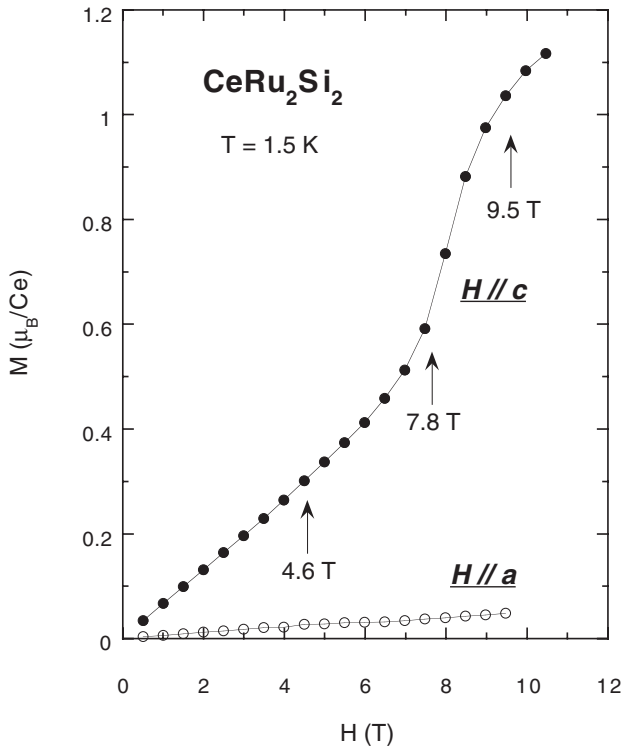

Figure 1. Magnetization curves of the $CeRu_2Si_2$ single crystal used for polarized neutron experiments at $T = 1.5$ K up to $H = 10$ T. The arrows indicate the three different fields of the measurements.

value of $F_M(0\,0\,0)$ is the magnetization measured in the same experimental conditions. The 3D density has been reconstructed by calculating a map on $64 \times 64 \times 124$ pixels. This 3D map can then be projected along any direction. Figure 2 shows the projections along the ***b***- and ***c***-axes, respectively, for the experiment in $H = 4.6$ T. On the two projected maps, one can see that no magnetization is found on the Ru or Si sites but that all the moment is located on the Ce atoms. The observed shape of this magnetization distribution looks quite circular. However, the density projected along the ***b***-axis is slightly elongated along the ***a***-direction. The results obtained for the two other applied magnetic fields are similar.

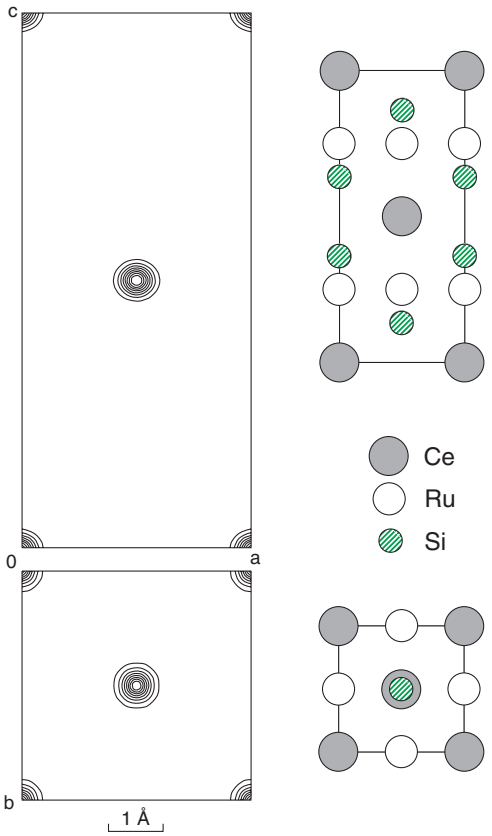

Figure 2. Magnetization distribution obtained with MaxEnt for $CeRu_2Si_2$ in an applied magnetic field of 4.6 T. The top and bottom parts are the projections along the ***b***- and ***c***-axes, respectively. The separation between the contour lines is 0.143 μ_B Å^{-2}. On the right-hand side is a schematic representation of the corresponding projected crystal structure.

(This figure is in colour only in the electronic version)

As the whole magnetic density can be attributed to the cerium, the dependence in the reciprocal space of the experimental Ce magnetic amplitudes $\mu f(\boldsymbol{Q})$ is directly obtained from $F_M(\boldsymbol{Q})$ (μ is the 4f magnetic moment, and $f(\boldsymbol{Q})$ is the magnetic form factor for the scattering vector $\boldsymbol{Q}$, with $|\boldsymbol{Q}| = 4\pi(\sin\theta/\lambda)$). This is drawn for the three different applied fields in figure 3. As can be expected from the magnetization curves, the higher the applied field, the higher these amplitudes are. The Ce form factors at each field $f(\boldsymbol{Q})$ are compared in figure 4. They present quite similar $\boldsymbol{Q}$ dependences.

4. Data analysis

Knowing the $4f^1$ wavefunctions $|\psi\rangle = \sum_M a_M |J, M\rangle$, the Ce form factor $f(\boldsymbol{Q})$ can be calculated by the tensor-operator method [17] with the radial integrals tabulated in [18]. In the presence of the crystal electric field of quadratic symmetry, the Ce^{3+} ion ground multiplet $J = 5/2$ is split into three doublets. For a field applied along a fourfold quantization axis of the structure, the only possible M values have to follow $\Delta M = \pm 4$. The wavefunctions of the doublets are then of type $|\psi\rangle = a_1 |5/2, \pm 5/2\rangle + a_2 |5/2, \mp 3/2\rangle$, $|\psi\rangle = a_2 |5/2, \pm 5/2\rangle - a_1 |5/2, \mp 3/2\rangle$ and $|\psi\rangle = |5/2, \pm 1/2\rangle$.

Refinements on the experimental values of $\mu f(\boldsymbol{Q})$ were undertaken for the three experiments. Because of the low temperature of the measurements, only the ground doublet was considered. The results show that the Ce wavefunction is, in the three cases, almost of pure

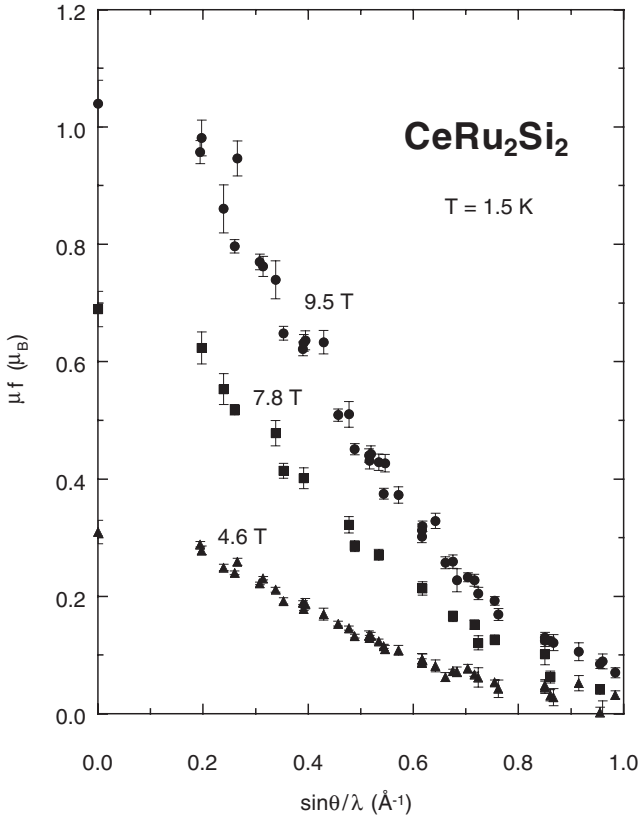

Figure 3. Magnetic amplitudes $\mu f(\boldsymbol{Q})$ measured at $T = 1.5$ K in different applied magnetic fields.

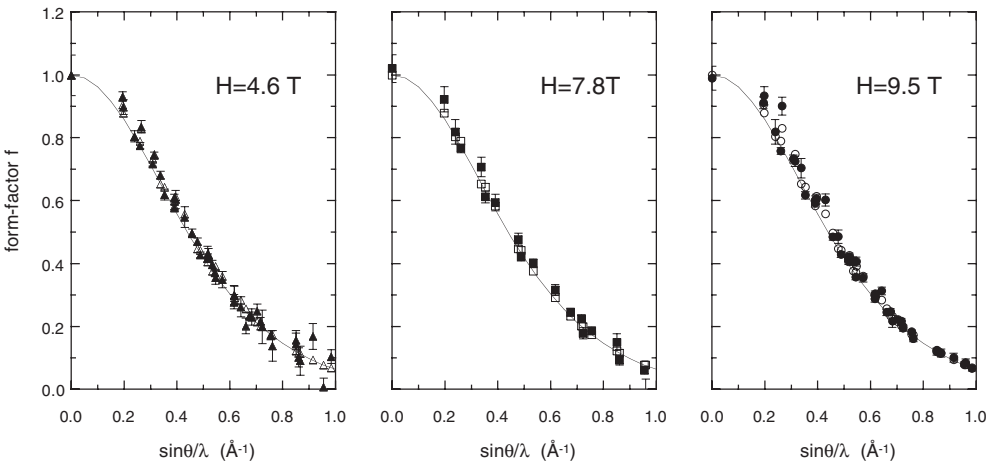

Figure 4. Comparison of the magnetic form factors $f(\boldsymbol{Q})$ in three different magnetic fields. The full symbols represent experimental points and the open symbols calculated points. The full curve represents the calculated form factor for the reflections $(h\,k\,0)$ of the equatorial plane.

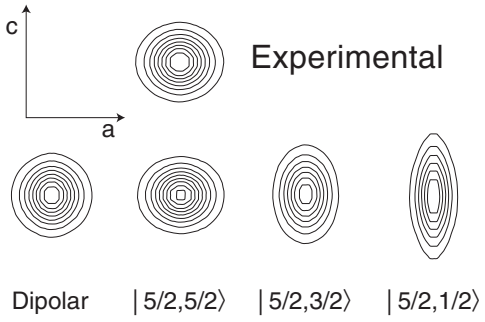

Figure 5. Comparison of the observed density projected along the ***b***-axis with those calculated, in the same way in the dipolar approximation and for the three basic 4f wavefunctions of cerium.

$|5/2, 5/2\rangle$-type, the highest value obtained for the $|5/2, 3/2\rangle$-type term being $0.03(\pm 0.12)$. This result is in agreement with the shape of the magnetization distribution found on the MaxEnt maps (figure 2). In figure 5, the observed density projected along the ***b***-axis is compared to those calculated in the same way (MaxEnt with same $(h\,k\,l)$ and same error bars) for a pure spherical density (dipolar approximation), and for the three basic 4f wavefunctions ($|5/2, 5/2\rangle$, $|5/2, 3/2\rangle$ and $|5/2, 1/2\rangle$). Only the density corresponding to the $|5/2, 5/2\rangle$ wavefunction is oblate [19], slightly elongated along the ***a***-axis and similar to the observed density.

We have therefore assumed that the fundamental state of the Ce^{3+} ion is a $|5/2, \pm 5/2\rangle$ doublet. It is split by the magnetic field into two levels separated by an energy $\triangle$, which increases with the applied field. The magnetic form factor $f(\boldsymbol{Q})$, as well as the resulting 4f moment μ, associated with each wavefunction, can be calculated and the resulting values for the doublet are obtained by thermal averaging at $T = 1.5$ K. The calculated values of the form factor are compared to the experimental values in figure 4. As the oblate magnetic density presents a cylindrical symmetry, the calculated form factor for the reflections $(h\,k\,0)$ of the equatorial plane can be represented by a full curve lying below the values for the other reflections (figure 4). The values of the splitting $\triangle$ for each experiment are given in table 3. The calculated 4f moment μ is compared to the measured magnetization. For each applied field, their values are the same, leading to the conclusion that, whatever the magnetic state of the compound, no polarization of the conduction electrons has been observed and the moment is only of 4f character.

Table 3. Splitting $\triangle$ of the ground doublet and corresponding 4f moment μ compared to the measured magnetization, in the three different applied fields.

H (T)	$\triangle$ (K)	Calculated 4f moment μ (μ_B)	Magnetization (μ_B/Ce)	R (%)	χ^2
4.6	0.437	0.31	0.31(2)	3.2	1.3
7.8	0.98	0.68	0.69(3)	5.9	1.9
9.5	1.61	1.05	1.04(4)	4.0	1.7

5. Discussion

Our polarized neutron experiments aimed to characterize the magnetic state on both sides of the metamagnetic transition of $CeRu_2Si_2$. Such a measurement allows us to separate the different contributions to the magnetization density: the localized 4f contribution and the polarization of the conduction electrons. Both contributions are generally observed in anomalous rare-earth compounds, the magnetization being predominantly of 4f character [19–22].

In $CeRu_2Si_2$, only the localized 4f contribution is found. The wavefunction has an almost pure $|5/2, 5/2\rangle$ ground state for any applied magnetic field. Until now, information on the crystal field scheme of $CeRu_2Si_2$ was only provided by bulk measurements (specific heat and susceptibility). The present determination is compatible with these previous analyses [23–25] which showed a dominant $|5/2, 5/2\rangle$ contribution with $0.96 \leqslant a_1 \leqslant 1$. It is worth underlining that INS experiments do not show evidence of well-defined crystal field levels because of a large broadening due to the Kondo effect [26].

Our data show no change in the localization of the magnetization under the external magnetic field. Only a nonlinear variation of the moment is observed, thus extending the bulk data to non-zero $\boldsymbol{Q}$ values. This continuous behaviour can be directly compared with NMR/NQR data. Although the resonance techniques probe non-f sites, contrary to neutron scattering, it is known that conduction electron relaxation reflects the f-electron susceptibility [27]. In $CeRu_2Si_2$, resonance experiments show that the hyperfine coupling constant is the same at 4.8 and 10.7 T suggesting no drastic changes of the electronic properties near H_m [5, 6] in complete agreement with our present microscopic experimental results. To a lesser extent, such a conclusion is indirectly made for most bulk measurements. Only quantum oscillation experiments have been interpreted by a drastic change of the nature of 4f electrons at the metamagnetic transition. Such a conclusion is intimately linked to the question of the formation of heavy quasi-particle bands in these systems and deserves more theoretical attention. Previously, several theoretical approaches have attempted to describe the metamagnetic behaviour of $CeRu_2Si_2$. Beyond the Kondo impurity models, magnetic interactions must be taken into account since INS revealed the switching of magnetic interaction from antiferromagnetic to ferromagnetic [7]. Such considerations have recently been taken into account in a new model where magnetic interactions evolve under a magnetic field. This reflects the field evolution of the 'camel-back' structure of the density of states proposed for $CeRu_2Si_2$ [28]. The duality model of the HF [29] also describes the metamagnetic behaviour. This model, which takes into account both the itinerant and localized character of HF compounds, could naturally explain the differences observed using different probes. On the one hand, resonance techniques and neutron scattering show evidence that the dominant magnetic contribution is 4f. On the other hand, quantum oscillation measurements show the necessity that the 4f electrons participate in the Fermi surface, via a very narrow band related to their localized character.

6. Conclusion

Our polarized neutron diffraction results provide new microscopic experimental evidence for the absence of a change of nature of the 4f electrons at the metamagnetic transition of $CeRu_2Si_2$, while there is a collapse of antiferromagnetic correlations and an emergence of ferromagnetism above H_m. Our data show that the wavefunction is almost pure $|5/2, 5/2\rangle$ and does not evolve with the magnetic field. This is in agreement with the NMR/NQR result which shows no change of the hyperfine coupling coefficient versus magnetic field.

Acknowledgments

We acknowledge S Kambe, K Ishida and T Kohara for discussions of the numerous NMR/NQR results.

References

[1] Kuramoto Y and Kitaoka Y 2000 *Dynamics of Heavy Electrons* (Oxford: Oxford University Press)
[2] Flouquet J, Kambe S, Regnault L-P, Haen P, Brison J-P, Lapierre F and Lejay P 1995 *Physica* B **215** 77
[3] Aoki H, Uji S, Albessard A K and Onuki Y 1993 *Phys. Rev. Lett.* **71** 2110
[4] Kambe S, Flouquet J, Haen P and Lejay P 1996 *J. Low Temp. Phys.* **102** 477
[5] Ishida K, Kawasaki Y, Kitaoka Y, Asayama K, Nakamura H and Flouquet J 1998 *Phys. Rev.* B **57** 11054
[6] Matsuda K, Kohori Y, Kohara T and Fujiwara K 2000 *J. Phys.: Condens. Matter* **12** 2061
[7] Raymond S, Regnault L-P, Kambe S, Flouquet J and Lejay P 1998 *J. Phys.: Condens. Matter* **10** 2363
[8] Lejay P, Muller J and Argoud R 1993 *J. Cryst. Growth* **130** 238
[9] Wolfers P 1990 *J. Appl. Crystallogr.* **23** 554
[10] Sears V F 1992 *Neutron News* **3** 26
[11] Becker P and Coppens P 1974 *Acta Crystallogr.* A **30** 129
[12] Bonnet M, Delapalme A, Becker P and Fuess H 1976 *Acta Crystallogr.* A **32** 945
[13] Boucherle J-X and Schweizer J 1981 *J. Magn. Magn. Mater.* **24** 308
[14] Papoular R J and Gillon B 1990 *Europhys. Lett.* **13** 429
[15] Papoular R J, Zheludev A, Ressouche E and Schweizer J 1995 *Acta Crystallogr.* A **51** 295
[16] Zheludev A, Papoular R J, Ressouche E and Schweizer J 1995 *Acta Crystallogr.* A **51** 450
[17] Lovesey S W and Rimmer D E 1969 *Rep. Prog. Phys.* **32** 333
[18] Freeman A J and Desclaux J-P 1979 *J. Magn. Magn. Mater.* **12** 11
[19] Boucherle J-X, Givord D and Schweizer J 1982 *J. Physique* C **7** 199
[20] Stassis C, Loong C K, Harmon B N, Liu S H and Moon R M 1979 *J. Appl. Phys.* **50** 7567
[21] Vrtis M L, Loong C K, Hinks D G, Stassis C and Arthur J 1987 *J. Appl. Phys.* **61** 3174
[22] Stassis C, Arthur J, Majkrzak C F, Axe J D, Batlogg B, Remeika J, Fisk Z, Smith J L and Edelstein A S 1986 *Phys. Rev.* B **34** 4382
[23] Besnus M-J, Kappler J-P, Lehmann P and Meyer A 1985 *Solid State Commun.* **55** 779
[24] Voiron J, Mignot J-M, Lejay P, Haen P and Flouquet J 1988 *J. Physique* **49** 1555
[25] Fischer G and Herr A 1987 *Phys. Status Solidi* b **141** 589
[26] Severing A, Holland-Moritz E, Rainford B D, Culverhouse S R and Frick B 1989 *Phys. Rev.* B **39** 2557
[27] Evans S M M and Coqblin B 1991 *Phys. Rev.* B **43** 12 790
[28] Satoh H and Ohkawa F J 2001 *Phys. Rev.* B **63** 184401
[29] Miyake K and Kuramoto Y 1990 *J. Magn. Magn. Mater.* **90–91** 438